HEMISPHEROIDAL SINGLE-PARTICLE SHELL MODEL

D.N. Poenaru, R.A. Gherghescu, A.V. Solov'yov, W. Greiner,

Hemispheroidal quantum harmonic oscillator,

Physics Letters A **372** (2008) 5448-5451.

OUTLINE

- Experimental mass spectrum of free metallic clusters
- Neutral free spheroidal Na cluster
- Atomic clusters on planar surfaces
- Hemisphere and Hemispheroidal shapes
- Deformed single particle shell models
  - Spheroidal harmonic oscillator
  - Hemispheroidal harmonic oscillator
  - Influence of the $\mathbf{l}^2$ term
- Conclusions

Macroscopic-Microscopic meth.

LDM and the shell correction method used in Nuclear Physics are suitable since delocalized conduction electrons of a metallic cluster form a Fermi liquid like the nucleons.

- Liquid Drop Model deformation energy: E_{LD}
- Single-particle shell model (SPSM): energy levels vs. deformation generally time consuming computations
- Shell corrections: δE
- Total deformation energy: $E_{def} = E_{LD} + \delta E$

for an eq. of the drop surface $\rho = \rho(z)$. The potential part of SPSM Hamiltonian should admit $\rho = \rho(z)$ as an equipotential surface. We choose the hemispheroidal shape, allowing to obtain analytical results — computational time negligible.

EXP: Prolate clusters on a surface

Ultrasensitive microscopy: Scanning tunneling microscope (STM) — 1981 Gerd Binnig and Heinrich Rohrer (Nobel Prize 1986). Atomic Force Microscope (AFM), etc.

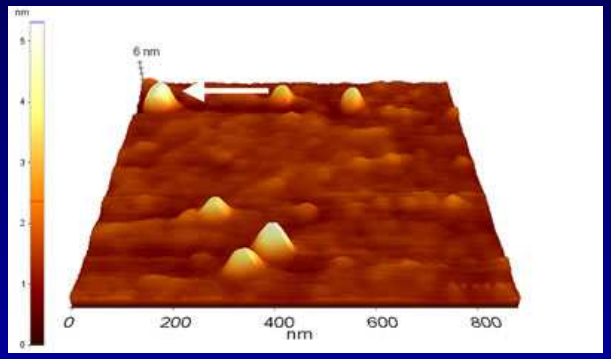

Au colloids deposited on a special glass. B. Bonanni and S. Cannistraro, *J. Nanotechnology Online*, Nov. 11, 2005. DOI: 10.2240/azojono0105.

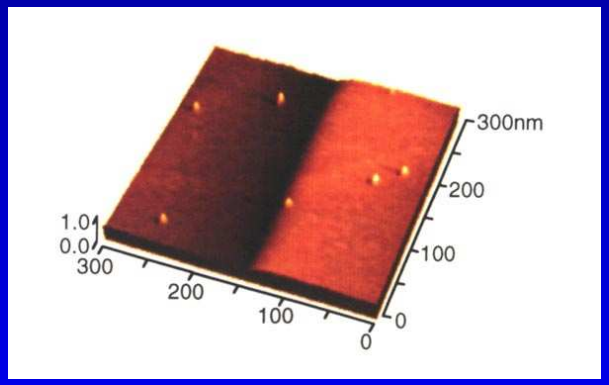

Clusters projected with energy close to the threshold stay at the impact point. Loughborough University & University of Birmingham.

Oblate clusters on a surface

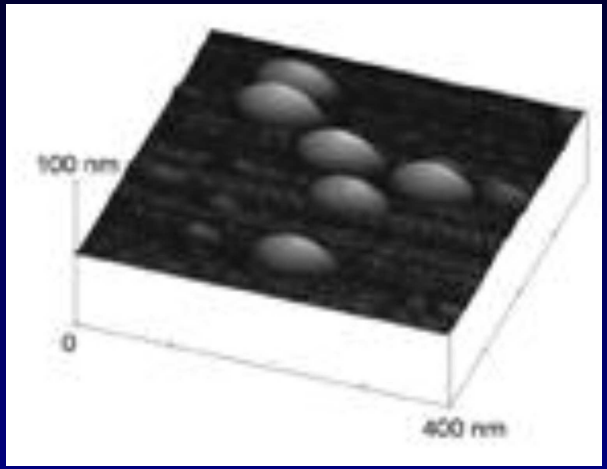

AFM image of Bi clusters supported on a SiO_2 surface. J.C. Partridge, S.A. Brown *et al., Phys. Stat. Sol. (a)* **203** (2006) 1217

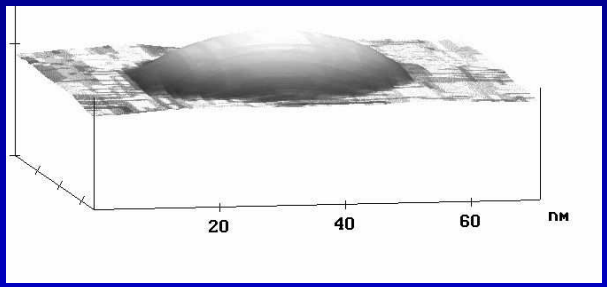

One of the cluster from the above figure. Simon A. Brown, private communication, 2008

Mass spectrum Na free clust.

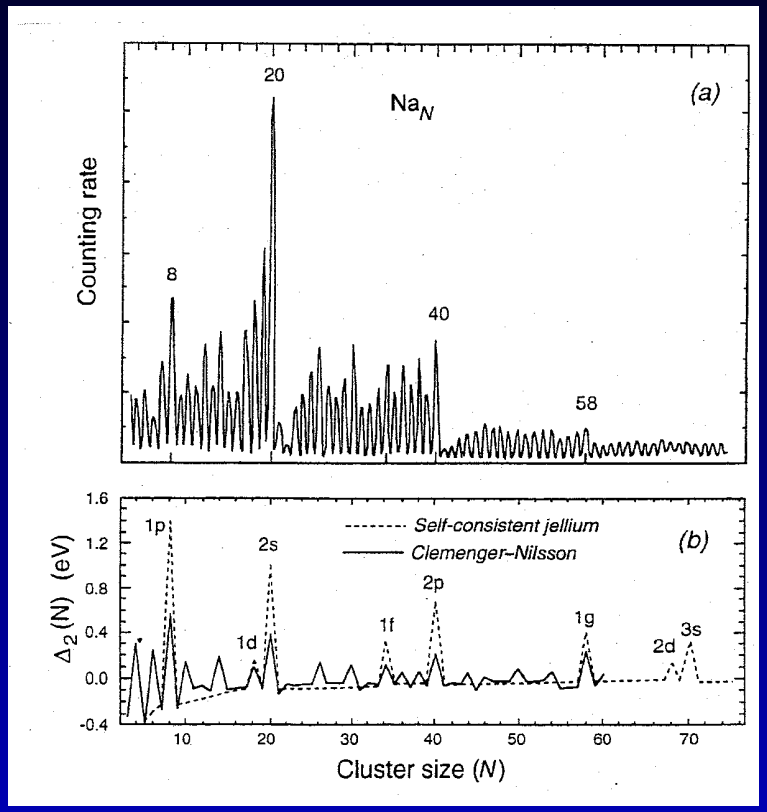

(a) Mass spectrum detected with a quadrupole mass analyser. Major peaks at **8, 20, 40, 58.**

(b) Calculated 2nd differences in total electronic energies.

Next magic numbers: **92, 136, 198, 264, 344, 442, ...**

From W. D. Knight *et al. Phys. Rev. Lett.* **52** (1984) 2141–2143.

Surface parametrization

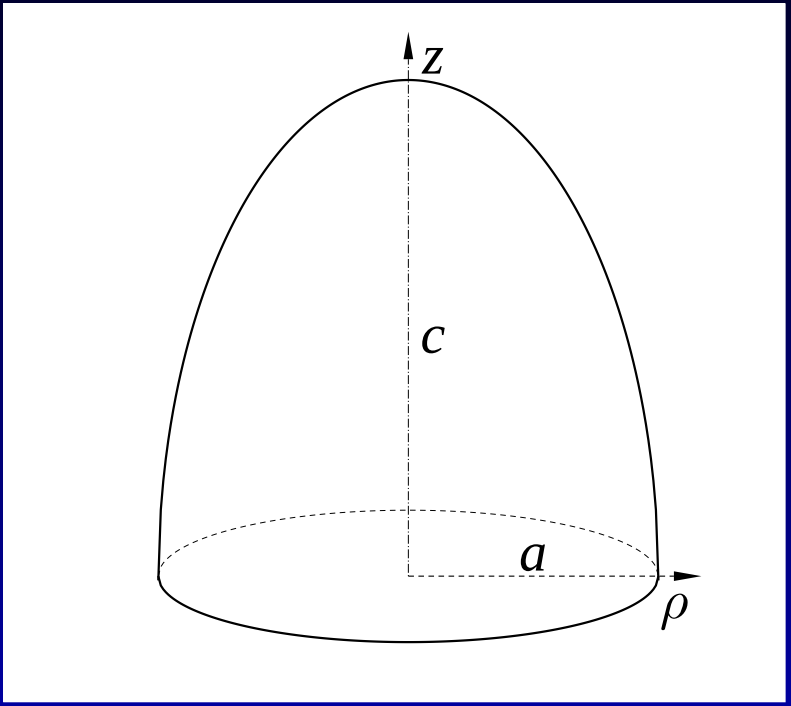

Hemispheroid with z-axis $\perp$ on the surface plane

$$\rho^2 = \begin{cases} (a/c)^2(c^2 - z^2) & z \geq 0 \\ 0 & z < 0 \end{cases}$$

$c > a$ **– prolate**

$c < a$ **– oblate**

D.N. Poenaru, R.A. Gherghescu, A.V. Solov'yov, W. Greiner,
Europhysics Letters **79** (2007) 63001.
D.N. Poenaru, R.A. Gherghescu, I.H. Plonski, A.V. Solov'yov, W. Greiner,
Europ. Phys. J. D **47** (2008) 379-393. *HIGHLIGHT PAPER.*
D.N. Poenaru, R.A. Gherghescu, A.V. Solov'yov, W. Greiner,
Phys. Lett. A **372** (2008) 5448-5451.

Spheroidal deformation

Spheroidal deformation δ

$\delta < 0$ oblate $\quad$ $\delta > 0$ prolate

(K.L. Clemenger, PhD Thesis, Univ. of California, Berkeley, 1985)

Dimensionless semiaxes (units of $R_0 = r_s N^{1/3}$ for spheroid and of $R_s = 2^{1/3} R_0$) for hemispheroid

$$a = \left(\frac{2-\delta}{2+\delta}\right)^{1/3} \quad ; \quad c = \left(\frac{2+\delta}{2-\delta}\right)^{2/3}$$

$$\frac{a}{c} = \frac{2-\delta}{2+\delta} = a^3$$

r_s – Wigner-Seitz radius. N – number of atoms (delocalized conduction electrons for monovalent metals.)

Short Spheroidal Cap, $h < c$

Shape independent variables: δ , d_0

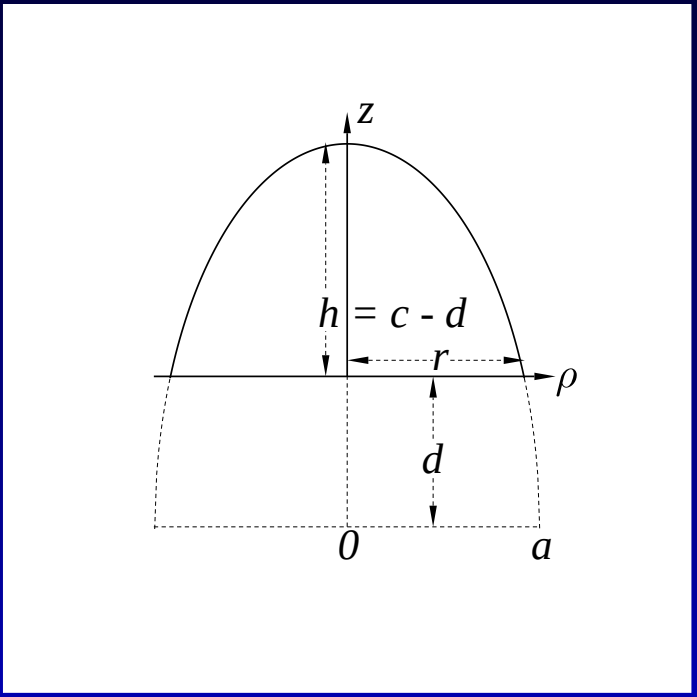

$$\rho^2 = \begin{cases} (a/c)^2(c^2 - z^2) & z \geq d \\ 0 & z < d \end{cases}$$

lengths in units of

$R_s = 4^{1/3} r_s N^{1/3} [h_0^2(3 - h_0)]^{-1/3}$

given $d_0 = d(\delta = 0)$

$h_0 = 1 - d_0$

$r_0 = \sqrt{1 - d_0^2}$

$r^2 = (a/c)^2(c^2 - d^2)$ Volume conservation leads to

$h^3 - 3ch^2 + c^3 h_0^2(3 - h_0) = 0$ with a real solution $h = ch_0$

Long Spheroidal Cap, $h > c$

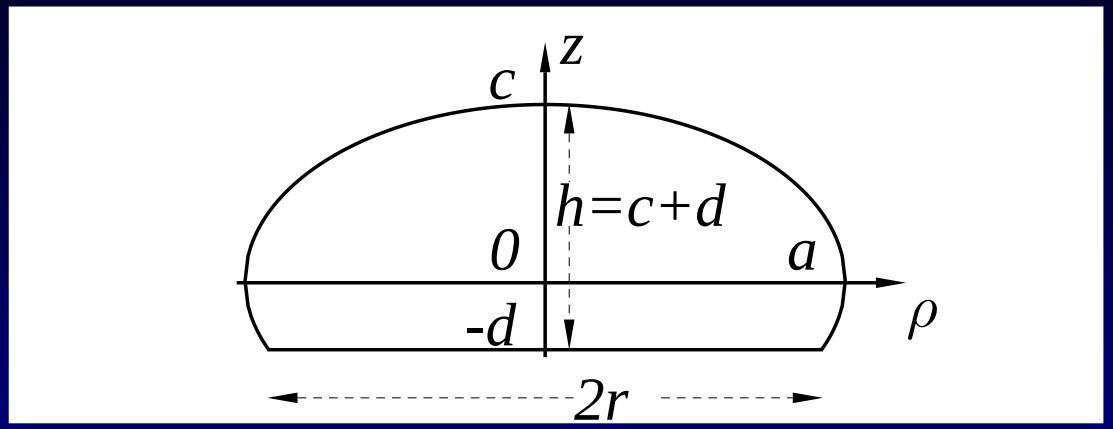

$$\rho^2 = \begin{cases} (a/c)^2(c^2 - z^2) & z \geq -d \\ 0 & z < -d \end{cases}$$

lengths in units of $R_s = 4^{1/3} r_s N^{1/3} [h_0^2(3 - h_0)]^{-1/3}$

given $d_0 = d(\delta = 0),\ h_0 = 1 + d_0,\ r_0 = \sqrt{1 - d_0^2}$

$r^2 = (a/c)^2(c^2 - d^2) \qquad h = ch_0$

Spherical shell model

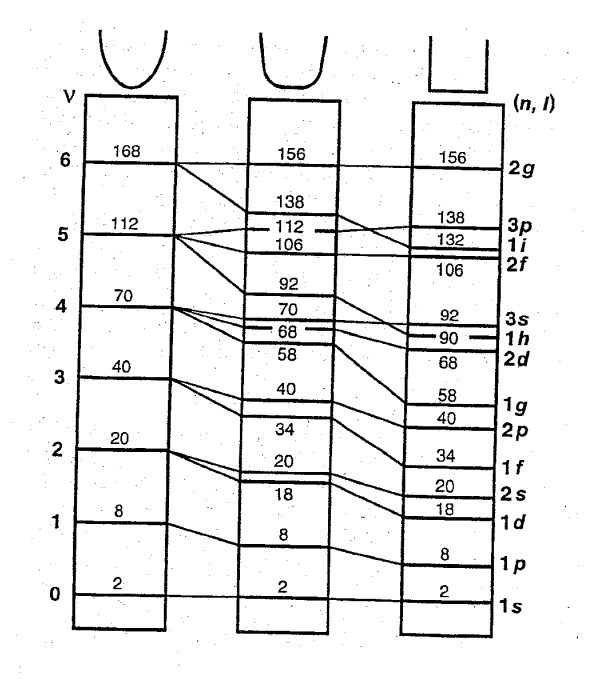

letter	name	l
s	sharp	0
p	principal	1
d	diffuse	2
f	fundamental	3
g		4
h		5
	etc	

Spectroscopic notation of clusters follows that of nuclei. The letters s, p, d, ... are associated to angular momentum **l**.

The spectrum depends on the well shape. High l states probe mainly the outer regions of the potential (centrifugal effects). The sensitivity to the details of the potential is greatest for higher energy electrons, because the electronic wavelengts are smaller for those energy levels.

Jahn-Teller effect (studied for nuclei by Nilsson): for open shell clusters (which are degenerate in their spherical state), the total energy can be lowered by distorting the cluster (lifting the degeneracy).

Spheroidal harmonic oscillator I

The harmonic oscillator (HO) potential part of the Clemenger-Nilsson model (K.L. Clemenger, *Phys. Rev. B* **32** (1985) 1359)

$$V = \frac{MR_0^2}{2}(\omega_\perp^2\rho^2+\omega_z^2z^2) = \frac{M\omega_0^2R_0^2}{2}\left[\rho^2\left(\frac{2+\delta}{2-\delta}\right)^{2/3} + z^2\left(\frac{2-\delta}{2+\delta}\right)^{4/3}\right]$$

The eigenvalues of the 3-dimensional Hamiltonian are

$$E = \hbar\omega_\perp(n_\perp+1) + \hbar\omega_z\left(n_z+\frac{1}{2}\right)$$

The main quantum number $n = n_\perp + n_z$. In units of $\hbar\omega_0$

$$\epsilon = \frac{\mathbf{E}}{\hbar\omega_0} = \frac{\mathbf{2}}{(\mathbf{2}-\delta)^{\mathbf{1/3}}(\mathbf{2}+\delta)^{\mathbf{2/3}}}\left[\mathbf{n}+\frac{\mathbf{3}}{\mathbf{2}}+\delta\left(\mathbf{n}_\perp-\frac{\mathbf{n}}{\mathbf{2}}+\frac{\mathbf{1}}{\mathbf{4}}\right)\right]$$

Spheroidal HO II

The single-particle shell gap (K.L. Clemenger, 1985):

$$\hbar\omega_0 = \frac{49 \text{ eV bohr}^2}{r_s^2 N^{1/3}} \left[1 + \frac{t}{r_s N^{1/3}}\right]^{-2} = \frac{13.72 \text{ eV Å}^2}{r_s R_0} \left[1 + \frac{t}{r_s N^{1/3}}\right]^{-2}$$

r_s is the Wigner-Seitz radius (atomic units), t is the electronic spillout of the neutral cluster (we assume $t = 0$).

Levels are labeled by two quantum nbers $(n, n_\perp)$ — integers. For every $n = 0, 1, 2, ...$ one has $n_\perp = 0, 1, 2, ..., n$. Each level may accomodate $2n_\perp + 2$ particles. One has $(n + 1)(n + 2)$ atoms in a completely filled shell. The magic nbers for spherical shapes ($\delta = 0$) are $(n + 1)(n + 2)(n + 3)/3 = 2, 8, 20, 40, 70, 112, 168...$

Spheroidal HO energy levels

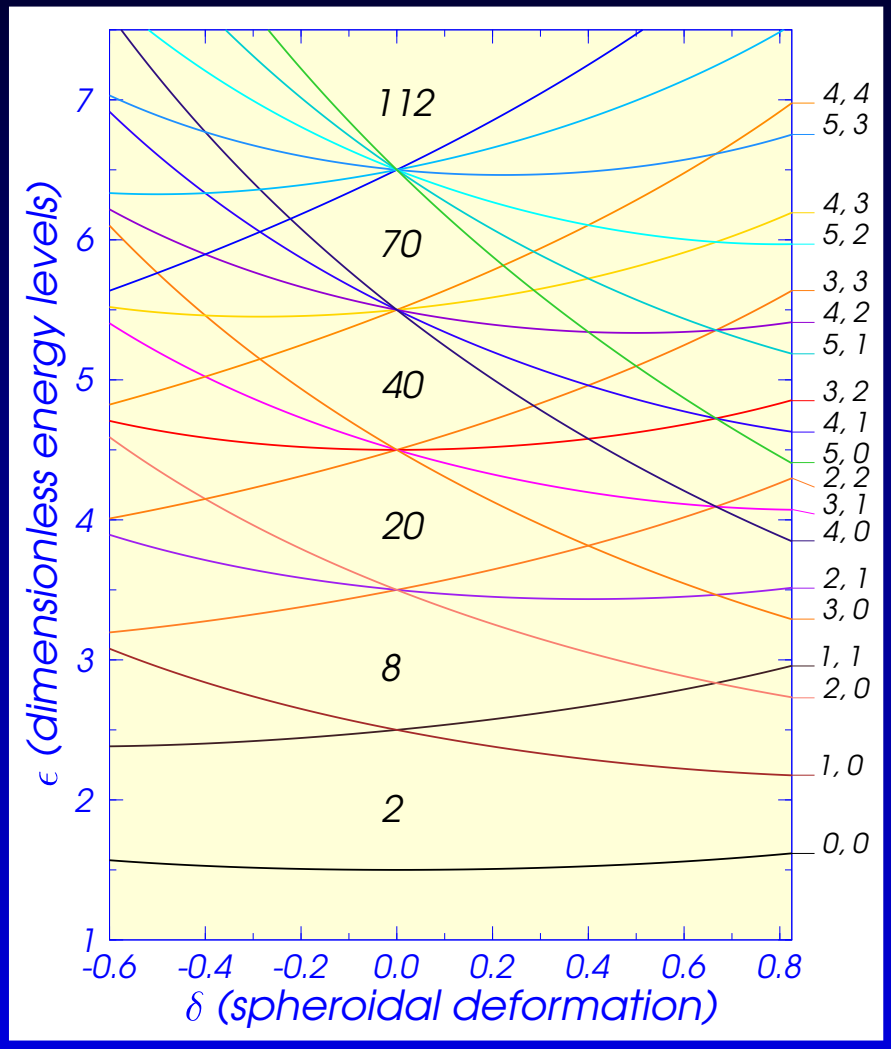

Label: $n, n_\perp$.

For $\delta > 0$ (prolate shape) at $n_\perp = 0$ the energy decreases with deformation, except for $n = 0$, $\epsilon(n_\perp = 0) = [2n+3-\delta(n-1/2)]/[(2-\delta)^{1/3}(2+\delta)^{2/3}]$

When $n_\perp = n$ it increases $\epsilon(n_\perp = n) = [2n+3+\delta(n+1/2)]/[(2-\delta)^{1/3}(2+\delta)^{2/3}]$

Remark a 2nd degeneracy at $\delta = 2/3$

Magic nbers of spheroidal HO

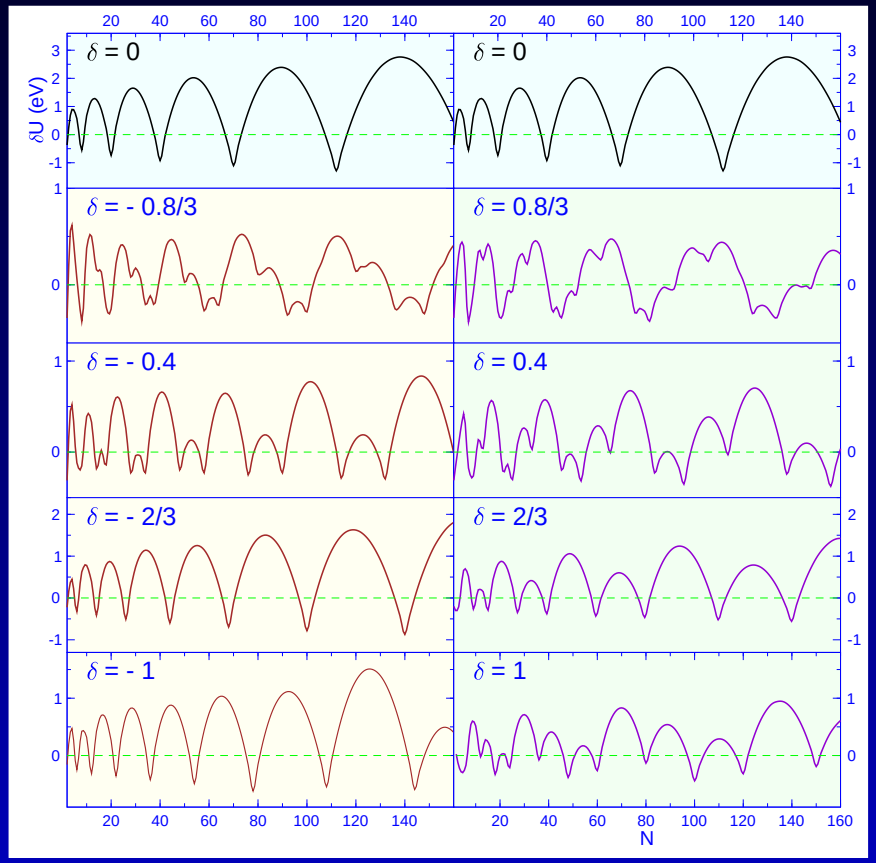

The spherical magic numbers $(n+1)(n+2)(n+3)/3$ are 2, 8, 20, 40, 70, 112, 168 ...

The magic numbers at the oblate spheroidal superdeformed shape ($\delta = -2/3$) are: 2, 6, 14, 26, 44, 68, 100, 140, ...

Magic nbers of spheroidal HO II

Sphere ($\delta = 0$): 2, 8, 20, 40, 70, 112, 168 ...

Oblate shapes:

$\delta = -0.8/3$ 2, 8, 18, 20, 34, 38, 58, 64, 92, 100, 136, 148,

$\delta = -0.4$ 2, 6, 8, 14, 18, 28, 34, 48, 58, 76, 90, 114, 132,

$\delta = -2/3$ 2, 6, 14, 26, 44, 68, 100, 140,

$\delta = -1$ 2, 6, 12, 22, 36, 54, 78, 108, 144,

Prolate shapes:

$\delta = 0.8/3$ 2, 8, 20, 22, 42, 46, 76, 82, 124, 134,

$\delta = 0.4$ 2, 8, 10, 22, 26, 46, 54, 66, 84, 96, 114, 138, 156,

$\delta = 2/3$ 2, 4, 10, 16, 28, 40, 60, 80, 110, 140,

$\delta = 1$ 4, 12, 18, 24, 36, 48, 60, 80, 100, 120, 150,

DEFORMED SINGLE PARTICLE HEMISPHEROIDAL SHELL MODEL

New (hemispheroidal) HO

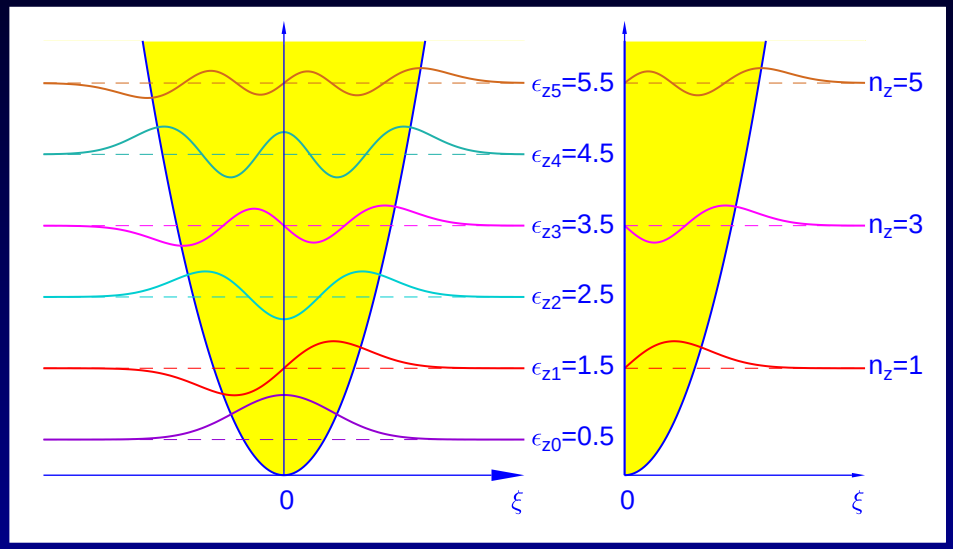

Axially-symmetric 3dim HO $H\Psi = E\Psi$

$H = T + V_\rho(\rho) + V_z(z)$

$\Psi = \psi^m_{n_r}(\eta)\Phi_m(\varphi)Z_{n_z}(\xi)$

$E_n = \hbar\omega_\perp(n_\perp + 1) + \hbar\omega_z(n_z + 1/2)$

The main quantum number $n = n_\perp + n_z = 0, 1, 2, 3, ...n$

$Z_{n_z}(\xi) = N_{n_z} e^{-\xi^2/2} H_{n_z}(\xi)$ $\xi = zR_0/\sqrt{\hbar/M\omega_z}$ - dim.less

N_{n_z} - ortonorm.constant Hermite polynomials with parity $(-1)^{n_z}$ meaning $H_{2n_z}(-\xi) = H_{2n_z}(\xi)$ and $H_{2n_z+1}(-\xi) = -H_{2n_z+1}(\xi)$. For hemispheroidal HO $V_z(0) \to \infty$. One should have $Z_{n_z}(\xi = 0) = 0$. **Only odd n_z values remain.**

Hemispheroidal HO en. levels

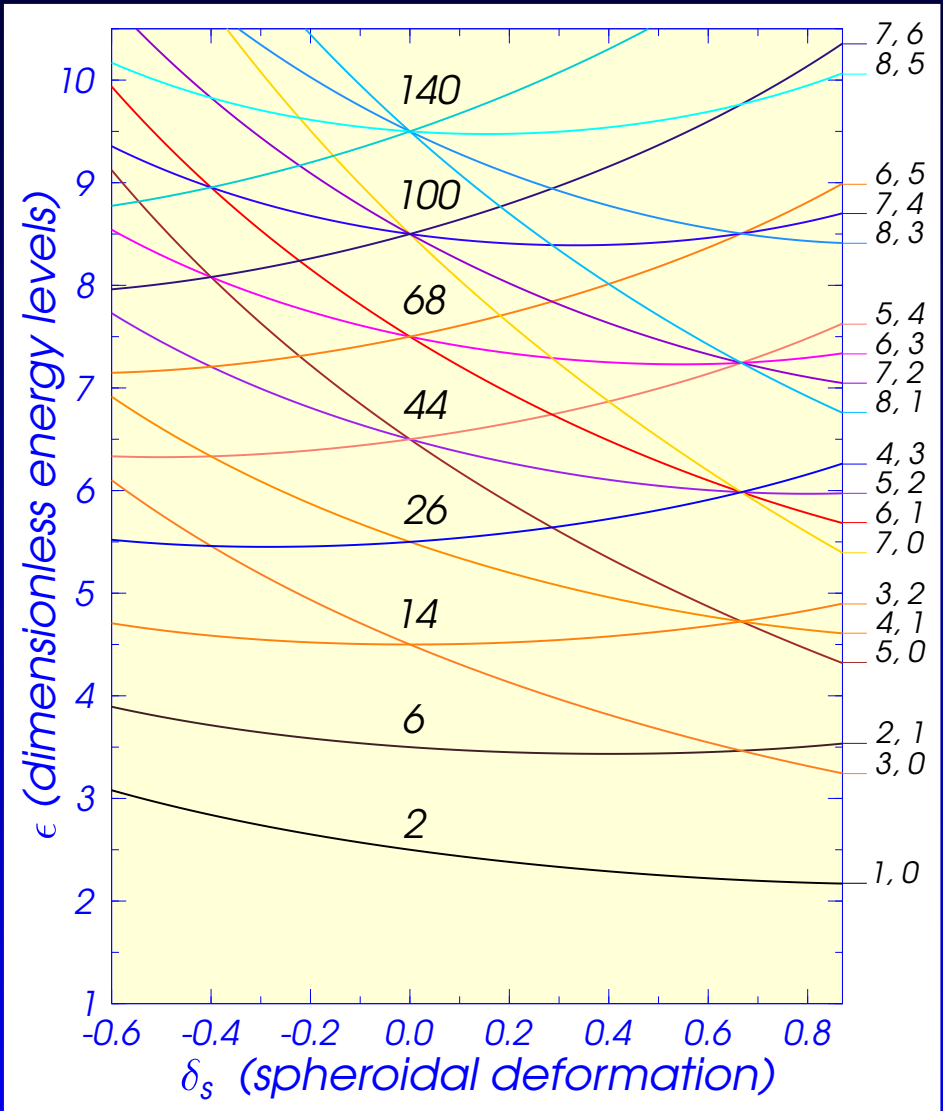

At every pair $(n, n_\perp)$, labeling an energy level, only those values are acceptable which lead to $n_z = n - n_\perp \geq 1$ — odd numbers.

The hemispherical magic numbers are equal to those obtained at the oblate spheroidal superdeformed shape, $\delta = -2/3$ i.e. 2, 6, 14, 26, 44, 68, 100, 140, ...

Magic nbers of hemispher. HO

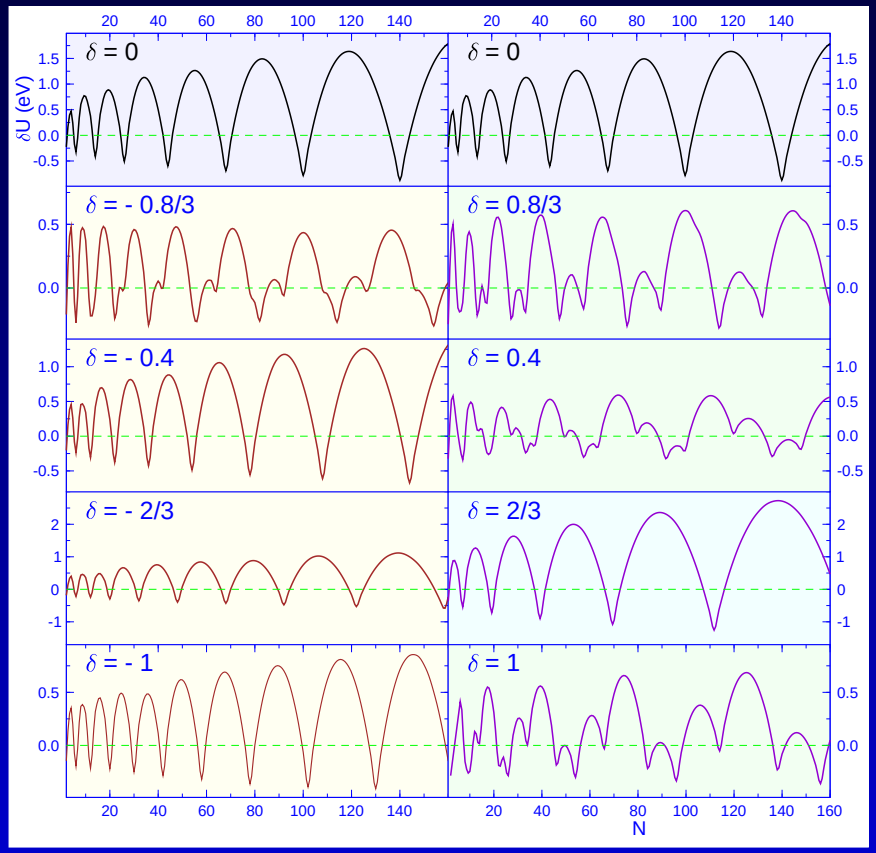

The contrib. to the hemispherical magic numbers of shells with:

(1) odd n: $(n+1)^2/2$,

(2) even n: $n(n+2)/2$.

Semi-spherical m.n. are identical to those obtained at the oblate spheroidal superdeformed shape ($\delta = -2/3$: 2, 6, 14, 26, 44, 68, 100, 140, ...)

Magic nbers of hemisph. HO II

Semi-sphere ($\delta = 0$): 2, 6, 14, 26, 44, 68, 100, 140, ...

Oblate hemispheroidal shapes:

$\delta = -0.8/3$ 2, 6, 12, 22, 26, 36, 42, 56, 64, 82, 92, 114, 126, 154,

$\delta = -0.4$ 2, 6, 12, 22, 36, 54, 78, 108, 144,

$\delta = -2/3$ 2, 6, 12, 20, 32, 48, 68, 92, 122, 158,

$\delta = -1$ 2, 6, 20, 30, 42, 58, 78, 102, 130,

Prolate hemispheroidal shapes:

$\delta = 0.8/3$ 2, 6, 8, 14, 18, 28, 34, 48, 58, 76, 90, 114, 132,

$\delta = 0.4$ 2, 8, 18, 20, 34, 38, 50, 58, 64, 80, 92, 100,

$\delta = 2/3$ 2, 8, 20, 40, 70, 112, 168,

$\delta = 1$ 2, 8, 10, 14, 22, 26, 46, 54, 66, 84, 96, 114, 138, 156,

Comparison of degeneracies

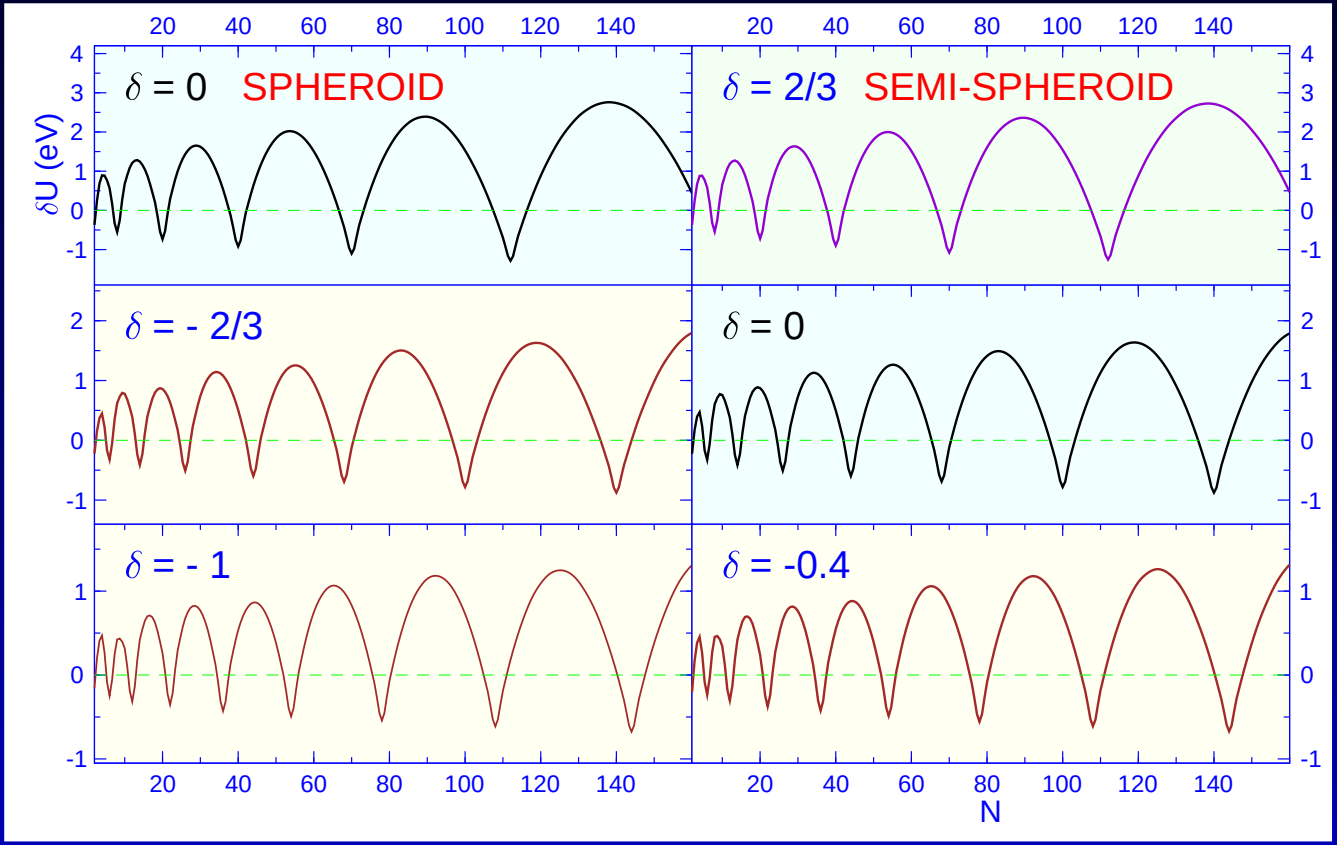

Striking: magic nbers at the prolate superdef. shape ($\delta = 2/3$) are identical to those obtained at the spherical shape

$(n+1)(n+2)(n+3)/3 =$ 2, 8, 20, 40, 70, 112, 168 ...

Influence of l^2 term (I)

$$H = -\frac{\hbar^2 \Delta}{2M} + V_{osc} - \hbar\omega_0 U(l^2 - \langle l^2 \rangle_n)$$

$$V_{osc} = \frac{M\omega_0^2 R_0^2}{2}\left(\frac{\rho^2}{a^2} + \frac{z^2}{c^2}\right) \quad U = 0.04 \text{ and } \langle l^2 \rangle_n = n(n+3)/2$$

$$\mathbf{l} = \nabla \mathbf{V_{osc}} \times \hat{\mathbf{p}} \quad l^2 = 0.5(l^+ l^- + l^- l^+) + l_z^2$$

$$\epsilon_{\mathbf{n}} = \frac{\mathbf{E_n}}{\hbar\omega_0} = \frac{\mathbf{n_\perp + 1}}{\mathbf{a}} + \frac{\mathbf{n_z + 1/2}}{\mathbf{c}} - \frac{\mathbf{U m^2}}{\mathbf{4a^4}} + \frac{\mathbf{Un(n+3)}}{\mathbf{2}}$$

$|m| = n_\perp - 2i \quad i = 0, 1, \ldots (n_\perp - 1)/2$ for odd $n_\perp$ or $(n_\perp - 2)/2$ for even $n_\perp$.

The possible nondiagonal terms coming from $(\hat{l}^+\hat{l}^- + \hat{l}^-\hat{l}^+)/2$ are not present since their contribution vanishes (n_z odd).

$|m| = (n_\perp - 2i)$ with $i = 0, 1, \ldots$ U — strength of interaction

Influence of l^2 term (II)

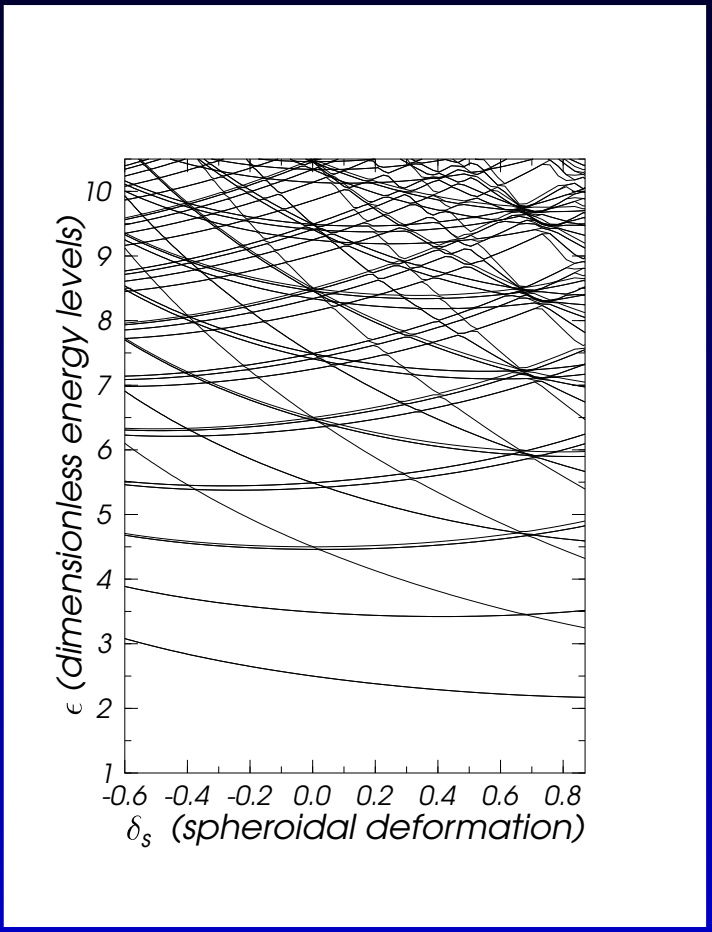

For lower levels (say up to 10 closed shells), the sequence of the magic numbers at the maximum degeneracy, $\delta = 2/3$, remain the same: $N = 2, 8, 20, 40, 70, 112, 168$. At very large oblate deformations, leading to "pan-cake" shapes approximating a 2D situation, one of the magic number is 6, in agreement with the experiments of Chiu et al.

Ya-Ping Chiu *et al.*, Magic Numbers of Atoms in Surface-Supported Planar Clusters, *Phys. Rev. Lett.* **97** (2006) 165504.

CONCLUSIONS

- Neutral, free hemispheroidal clusters were investigated, as a 1st approx. to study cluster deposition on a surface
- A new hemispheroidal harmonic oscillator was derived. $Z(z)$ component of wave function has negative parity
- Its hemispherical ($\delta = 0$) magic numbers are identical with those obtained at the oblate spheroidal superdeformed shape: 2, 6, 14, 26, 44, 68, 100, 140, ...
- Maximum degeneracy at superdeformed ($\delta = 2/3$) prolate shape. Magic numbers identical with those of the spherical shape: 2, 8, 20, 40, 70, 112, 168 ...
- Interesting coincidence: within the LDM the most stable shape is a superdeformed prolate hemispheroid